SPIDER model simulations of aircraft plume dilution

N. Dotzek*, S. Matthes, and R. Sausen
Deutsches Zentrum für Luft- und Raumfahrt (DLR), Institut für Physik der Atmosphäre, Oberpfaffenhofen, Germany

Keywords: Aircraft emissions, plume dilution, simplified chemistry, effective emission indices.

ABSTRACT: To include the effect of aircraft plume processes (effective emissions indices) in large scale chemistry transport models and climate-chemistry models, the instantaneous dispersion (ID) and single-plume (SD) approaches exist. We use the box model SPIDER to evaluate these two concepts. Its simplified NO_x-O_3 chemistry parameterises only the most relevant non-linear processes. SPIDER simulations for varying NO_x background reveal the largest difference between ID and SP approaches in clean-air conditions. For a NO_x background of ~0.2 nmol mol^{-1}, the ID and SP approaches result in aviation-induced O_3 changes of opposite signs. Hence, this transition regime may require more attention in plume parameterisations applied in global atmospheric models.

1 MOTIVATION

Emissions from aircraft impact on global climate (cf. Brasseur et al., 1998; IPCC, 1999; Sausen et al., 2005). They are usually implemented in General Circulation Models (CGM) or Chemistry Transport Models (CTM) by an instantaneous dispersion of emitted matter over the large-scale grid boxes. Following Petry et al. (1998), this is called the instantaneous dispersion (ID) approach. The ID approach neglects non-linear chemical conversion processes in the evolving single plume. To resolve these by a plume model is called the single plume, or SP approach. However, detailed SP chemical modelling is computationally too demanding, both for more complex principle studies of plume-plume interactions, and for operational implementation in large-scale models.

To improve the ID approach in GCMs, Effective Emission Indices (EEIs) can be used (e.g., Möllhoff, 1996; Petry et al., 1998). These, and several other approaches to the problem, e.g., by Meijer et al. (1997), Meijer (2001), Karol et al. (1997, 2000), Kraabøl et al. (2000), Kraabøl and Stordal (2000) and Franke et al. (2008) applied detailed chemistry schemes. A simplified model was presented and validated by Dotzek and Sausen (2007) to evaluate various EEI concepts, and to perform studies of multi-plume interactions. This paper aims to (1) to apply this box model with simplified chemistry, the SPIDER (SP-ID Emission Relations) model, to various NO_x backgrounds and (2) to identify those NO_x background concentrations where the application of a more sophisticated single-plume approach yields results different from instantaneous dispersion approach.

2 MODEL DESIGN

In this study we use the SPIDER model which is a box model applying a simplified scheme for non-linear ozone production by aircraft NOx emissions at cruise altitude. Motivated by the work by Petry et al. (1998) who applied a detailed chemistry scheme, we aim at computing plume dilution, and comparing of ID and SP results using a computationally efficient box model with greatly simplified chemistry. The resulting SPIDER model avoids explicit solution of the chemical rate equations. Chemistry enters the equations only in parameterized form by "dynamic forcing" terms, and the only species considered are NOx and O3. The model is described in more detail by Dotzek and Sausen (2007). The objectives were to apply the validated SPIDER model to multiple plume interactions or varying background NOx fields, and to eventually evaluate different EEI approaches.

* *Corresponding author:* Dr. Nikolai Dotzek, Deutsches Zentrum für Luft- und Raumfahrt (DLR), Institut für Physik der Atmosphäre, Oberpfaffenhofen, 82234 Wessling, Germany. Email: nikolai.dotzek@dlr.de

2.1 *SPIDER model setup*

The main process to be covered by the SPIDER model is the non-linear production of O_3 by aircraft NO_x emissions at cruise altitude. Hence, the system of equations includes only these two species.
The physical processes which are to be explicitly included in and resolved by the model within a typical GCM grid box volume are a) the emission of NO_x inside the GCM box, S_{NOx}, b) non-linear production of ozone, P_{O3}, and c) the decay of the NO_x and O_3 fields by conversion to reservoir species. For treatment of the SP approach, additionally the background (outer domain, superscript o) and plume fields (inner domain, superscript i) have to be integrated separately, and the entrainment of background matter by turbulent mixing at the growing-plume boundary enters the budget equations as another individual term.
As the SPIDER model equations are formulated for the plume dispersion regime (the far-field solution), they cannot resolve initial titration, which is a near-field plume process. The initial ozone level in the plume must be lowered slightly compared to the background state to provide the proper initialisation values for the early dispersion regime. Eqs. (1-4) specify the budget equations for the ID and SP concepts. Following the convention we denote extensive quantities by upper-case ($[NO_x]$ = mol, $[O_3]$ = mol) and intensive quantities by lower-case letters ($[no_x]$ = nmol mol^{-1}). Parameterisation of photochemical ozone production P_{O3} applied for both approaches is presented below.

2.1.1 *ID budget equations*

In the following equations for instantaneous dispersion, dt denotes the temporal derivative d/dt:

$$d_t\, NO_x = S_{NOx}\ \delta(t-t') - \frac{1}{\tau_{NOx}} NO_x \quad , \tag{1}$$

$$d_t\, O_3 = P_{O3}(no_x) \qquad - \frac{1}{\tau_{O3}} O_3 \quad . \tag{2}$$

The reference background state without aircraft emissions follows for $S_{NOx} \equiv 0$. The decay, or conversion of NO_x and O_3 to reservoir species, is modelled as an exponential decay with fixed half-time periods τ (τ_{NOx} = 10 days, τ_{O3} = 30 days, cf. Köhler and Sausen, 1994).

2.1.2 *SP budget equations*

In the single-plume equations, each species must be treated with one budget equation for the plume (superscript i) and the background (superscript o). As the box model reference volume is one GCM grid box, the computation of entrainment in Eqs. (3-4) is terminated as soon as the plume volume V^i is equal to the reference volume V_{GCM}.

$$d_t\, NO_x^{\,i} = S_{NOx}\ \delta(t-t') + NO_x^{\,o} / V^o\ d_t V^i - \frac{1}{\tau_{NOx}} NO_x^{\,i} \quad , \tag{3a}$$

$$d_t\, NO_x^{\,o} = \qquad - NO_x^{\,o} / V^o\ d_t V^i - \frac{1}{\tau_{NOx}} NO_x^{\,o} \quad , \tag{3b}$$

$$d_t\, O_3^{\,i} = P_{O3}(no_x^{\,i}) \qquad + \quad O_3^{\,o} / V^o\ d_t V^i - \frac{1}{\tau_{O3}} O_3^{\,i} \quad , \tag{4a}$$

$$d_t\, O_3^{\,o} = P_{O3}(no_x^{\,o}) \qquad - \quad O_3^{\,o} / V^o\ d_t V^i - \frac{1}{\tau_{O3}} O_3^{\,o} \quad . \tag{4b}$$

Eq. (3a) encompasses the case a fresh aircraft plume being emitted along the axis of an aged plume from another aircraft earlier on (cf. Kraabøl and Stordal, 2000; Dotzek and Sausen, 2007).

2.2 *Parameterisation of PO3(nox) terms*

As treated in detail by, e.g., Johnson and Rohrer (1995), Brasseur et al. (1996), Grooß et al. (1998), and Meilinger et al. (2001), the production of ozone does not only depend on NO_x concentrations, but is a highly variable function of other species like O_3 itself, H_2O, CO, hydrocarbons, state variables p, and T, and the actinic flux J. A perfect parameterisation in this multidimensional phase space is impossible, and likely has prevented earlier simplified chemistry studies of plume dilution. However, the objective in developing the SPIDER model was to allow for principal studies of plume dilution, plume interaction, and methods to derive EEIs. A parameterisation of O_3 production as a function of nitrogen oxides for some typical atmospheric conditions at cruise altitude following the data presented in the literature is possible. Aside from the NO_x concentration, also the solar elevation angle must be taken into account, in order to capture the diurnal cycle of photochemical ozone production. This non-linear production of ozone as a function of the ambient NO_x concentrations was parameterised by Dotzek and Sausen (2007) for the SPIDER model Eqs. (2) and (4), evaluating five different parameterisations of which curve D from the Brasseur et al. (1996) data was selected in the SPIDER model. It includes effects of the diurnal cycle, while the other curves are very similar in shape, and their variation comes mainly from different ambient chemical conditions. Note the non-linearity, or rather non-monotonicity, of all P_{O3} curves. Low and very high NO_x concentrations are characterized by ozone depletion, while the peak ozone production is found in the range of 0.15 to 0.27 nmol mol^{-1}. The similarity of the curves in the upper troposphere gives us confidence that the SPIDER parameterisation of P_{O3} is adequate for principal process studies.

2.3 *Experimental model set-up*

We perform a case study of ozone formation by an aircraft plume at about 10 km cruising altitude. This setting is similar to the original model cases of Möllhoff (1996) and was also used by Dotzek and Sausen (2007) to validate the SPIDER model. Without wind shear or cross-plume wind components, the exhaust of a typical B747 airplane is emitted as a line-source at 0800 LST (local solar time) in a V_{GCM} = 50 x 50 x 1 km^3 reference volume. Ambient conditions are mid-latitude summer, T = 218 K and p = 236 hPa (about 10 km above see level, ASL) in the North Atlantic flight corridor. The initial average values of NO_x and O_3 in the plume are chosen to be representative of the early dispersion regime (about 100 s after emission): for NO_x, 2.97 nmol mol^{-1} and for O_3 196.5 nmol mol^{-1} (Petry et al., 1998). Linear Gaussian plume growth is specified, so after t_{ref} = 18 h of dilution, the plume volume becomes equal to the reference volume V_{GCM}. The SPIDER model runs were performed for NO_x background concentrations of 0.05, 0.075, 0.1, 0.2, 0.5, 1, 2 and 3 nmol mol^{-1}, respectively. These cover the range from clean-air to strongly polluted environments.

3 RESULTS FOR VARYING BACKGROUND NOX

In order to compare individual approaches for above model cases the temporal evolution of aircraft-induced O_3 change is presented as absolute values and per kilometre plume length along the flight path. Fig. 1 shows results for 0.05, 0.1, 0.2 and 1 nmol mol^{-1} NO_x backgrounds. During the first few minutes after plume emission aircraft-induced ozone change is characterised by ozone titration within the plume due to very high NO_x concentration under all NO_x background conditions.

Both for the absolute change in O_3 and the change per kilometre flight path, it becomes obvious that the largest differences between the ID and SP approaches materialise for clean-air ambient conditions, that is, for NO_x background concentrations of less than about 0.1 nmol mol^{-1}. After an initial ozone titration in SP simulations, ozone production during the early phase (up to several hours) is higher in SP simulations, compared to ID calculations. More than 12 hours after emissions this changes, and finally ozone production in SP simulations is lower than in ID calculations.
For strongly polluted environments (1, 2, 3 nmol mol^{-1}, latter two not shown), the ID and SP simulations yield essentially identical results at the time when the plume attains the same volume as the GCM grid box. Interestingly, a transition regime can be identified for NO_x backgrounds of about 0.2 nmol mol^{-1}, in which the ozone productions of the ID and SP approaches at $t = t_{ref}$ are small, but have opposite signs. Here, during 24 hours after emission, the SP approach leads to a small net destruction of O_3, while the ID approach leads to ozone production with a magnitude considerably larger than the destruction evaluated from the SP approach. This opposite sign of ozone change between SP and ID approach prevails from 4 hours after emission onward.

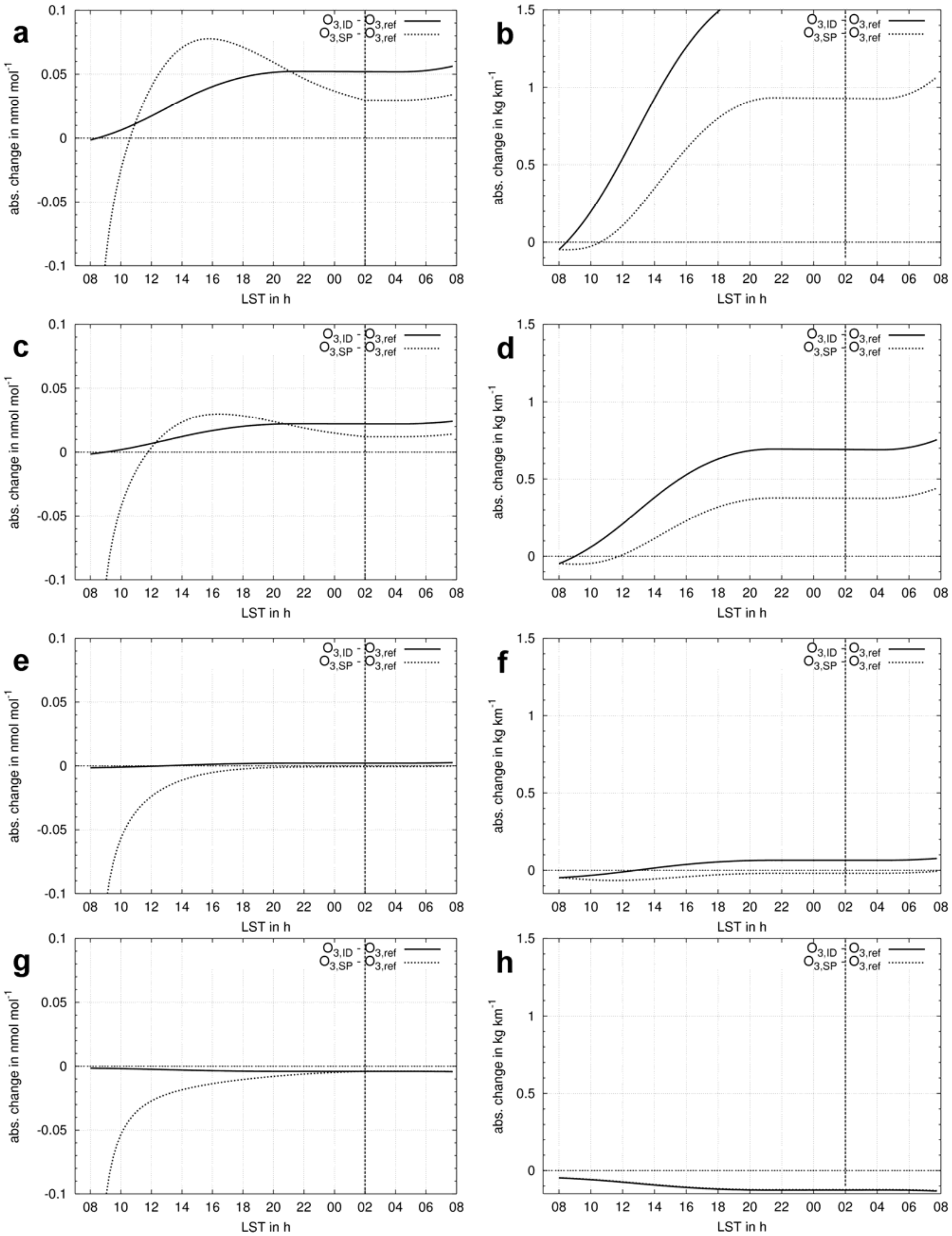

Figure 1. Aircraft-induced O_3 change as absolute change (left panels) and change per kilometre plume length along the flight path (right panels) compared to the background state for ID (solid) and SP simulations (dotted). Background NO_x concentrations increase from top to bottom: (a, b) 0.05 nmol mol^{-1}, (c, d) 0.1 nmol mol^{-1}, (e, f) 0.2 nmol mol^{-1}, and (g, h) 1 nmol mol^{-1}, Emission time was 0800 LST and after 18 h, the plume volume equals the GCM box volume (dashed line).

4 DISCUSSION

Depending on NO_x background concentrations, substantial differences between ID and SP approaches can occur. Differences in O_3 change observed in our results indicate that in the clean-air regime (below 0.1 nmol mol^{-1}) both ID and SP ozone productions are positive and show their largest absolute spreads. In the transition regime (~0.2 nmol mol^{-1}), an opposite sign can be observed between ID and SP approaches from several hours after emission on. This pattern prevails even after 18 hours of plume expansion to full GCM box volume. For more polluted regions, however, with NO_x backgrounds well above 0.2 nmol mol^{-1}, the ID and SP approaches yield increasingly similar results. Hence, for such conditions which can be found in the North Atlantic flight corridor, an ID approach may still be adequate and least time-consuming for application in GCMs or CTMs. Under clean-air conditions and in the transition regime, use of an ID approach would yield substantial differences from a more detailed SP approach, overestimating aviation-induced O_3 changes.

The simplifications made in the SPIDER model equations require some more discussion. The basic plume dilution processes were shown to be well-represented by Dotzek and Sausen (2007), in part even quantitatively. Some details are missing in the model which would require the complete set of chemical reactions – or an improved description of either the plume growth (being linear only on average, cf. Schumann et al., 1998) or the actinic flux in the P_{O3} term. Nonlinear plume growth already has been implemented as an option in the model, but to facilitate comparison to the Dotzek and Sausen (2007) results, it was not considered here. Our model set-up does not include a typical diurnal cycle. For the parametric functions of P_{O3}, a curve was selected from Brasseur et al. (1996) including a diurnal cycle. Future SPIDER versions will include a typical diurnal variation of these time scales, but this is a second-order effect with little consequence here.

For multi-plume interactions (Dotzek and Sausen, 2007), the net effect on the difference between ID and SP approaches critically depends on the age of the primary plume (and hence its NO_x and O_3 concentrations). Our present study with NO_x background variations across the whole GCM grid box, however, showed a consistent trend. The need for a more sophisticated description of plume processes in GCMs sets in at NO_x backgrounds of about 0.2 nmol mol^{-1}, first with a disparity of the signs of the (small) O_3 productions, and then with increasing magnitude for less polluted regions.

The inclusion of plume effects in the dispersion modelling of pollutants is not only relevant in aviation at cruise altitude, but also near the ground (Uphoff, 2008; Galmarini et al., 2008), for land transport (Ganev et al., 2008) and shipping (Franke et al., 2008). Several parameterisations to include these effects in mesoscale or general circulation models have been proposed recently. Cariolle et al. (2009) specifically addressed aircraft NO_x emissions in a similar setting as in out present paper. They track the plume air with NO_x concentrations above 1 nmol mol^{-1} by introducing a “fuel tracer” and a characteristic lifetime into their budget equations. Their detailed parameterisation confirms our results: Taking into account the plume processes consistently lowers the estimates of aircraft-induced O_3 production at cruise altitude in parts of the North Atlantic flight corridor.

5 CONCLUSIONS

Applying the SPIDER box model for various NO_x background concentrations illustrated:

- The largest differences between the ID and SP approaches occur for clean-air ambient conditions, that is, for NOx background concentrations of less than about 0.1 nmol mol-1;
- For strongly polluted environments, the ID and SP simulations yield essentially identical results at the time when the plume attains the same volume as the GCM grid box;
- A transition regime can be identified for NOx backgrounds of about 0.2 nmol mol-1 in which the ozone productions of the ID and SP approaches after 18 h are small, but have opposite signs.
- It appears necessary to also consider this transition regime in parameterisations of the ozone production by aircraft NOx emissions at cruise altitude, in addition to the clean-air regime.

Future work will encompass simulations for a wider range of likely environmental conditions at cruise altitude to assess the robustness of our findings.

6 ACKNOWLEDGMENTS

This work was partly funded by the European Commission FP6: ND and RS were supported by the Integrated Project QUANTIFY under contract no. 003893 (GOCE) and SM was supported by the Network of Excellence ECATS under contract no. ANE-CT-2005-012284.

REFERENCES

Brasseur, G. P., J.-F. Müller, and C. Granier, 1996: Atmospheric impact of NOx emissions by subsonic aircraft: A three-dimensional model study. J. Geophys. Res., 101 D, 1423-1428.

Brasseur, G. P., R. A. Cox, D. Hauglustaine, I. Isaksen, J. Lelieveld, D. H. Lister, R. Sausen, U. Schumann, A. Wahner, and P. Wiesen, 1998: European scientific assessment of the atmospheric effects of aircraft emissions. Atmos. Environ., 32(13), 2329-2418.

Cariolle, D., D. Caro, R. Paoli, D. A. Hauglustaine, B. Cuénot, A. Cozic, and R. Paugam, 2009: Parameterization of plume chemistry into large-scale atmospheric models: Application to aircraft NOx emissions. J. Geophys. Res., 114, D19302, doi:10.1029/2009JD011873.

Dotzek, N., and R. Sausen, 2007: SPIDER model process studies of aircraft plume dilution using simplified chemistry. In: Sausen, R., A. Blum, D.S. Lee and C. Brüning (eds.): Proceedings of an International Conference on Transport, Atmosphere and Climate (TAC). Luxembourg, Office for Official Publications of the European Communities, ISBN 92-79-04583-0, 261-266.

Franke, K.; V. Eyring, R. Sander, J. Hendricks, A. Lauer, and R. Sausen, 2008: Toward effective emissions of ships in global models. Meteorol. Z., 17(2), 117-129.

Galmarini, S., J.-F. Vinuesa, and A. Martilli, 2008: Modeling the impact of sub-grid scale emission variability on upper-air concentration. Atmos. Chem. Phys., 8, 141-158.

Ganev, K., D. Syrakov, Z. Zlatev, 2008: New parameterization scheme for effective indices for emissions from road transport. Ecol. Model., 217(3-4), 270-278.

Grooß, J.-U., C. Brühl, and T. Peter, 1998: Impact of aircraft emissions on tropospheric and stratospheric ozone. Part I: Chemistry and 2-D model results. Atmos. Environ., 32(18), 3173-3184.

IPCC, 1999: Aviation and the global atmosphere. – A special report of IPCC working groups I and III. (Penner, J. E., D. H. Lister, D. J. Griggs, D. J. Dokken, and M. McFarland (Eds.)). Intergovernmental Panel on Climate Change. – Cambridge University Press, Cambridge, UK and New York, NY, USA, 365 pp.

Johnson, C., and F. Rohrer, 1995: NOx and O3 chemistry in the upper troposphere and lower stratosphere. In: Schumann (1995), 325-335.

Karol, I. L., Y. E. Ozolin, and E. V. Rozanov, 1997: Box and Gaussian plume models of the exhaust composition evolution of subsonic transport aircraft in- and out of the flight corridor. Ann. Geophys. 15, 88-96.

Karol, I. L., Y. E. Ozolin, A. A. Kiselev, and E. V. Rozanov, 2000: Plume transformation index (PTI) of the subsonic aircraft exhausts and their dependence on the external conditions. Geophys. Res. Lett. 27(3), 373-376.

Kraabøl, A. G., and F. Stordal, 2000: Modelling chemistry in aircraft plumes 2: The chemical conversion of NOx to reservoir species under different conditions. Atmos. Environ. 34, 3951-3962.

Kraabøl, A. G., P. Konopka, F. Stordal, and H. Schlager, 2000: Modelling chemistry in aircraft plumes 1: Comparison with observations and evaluation of a layered approach. Atmos. Environ. 34, 3939-3950.

Köhler, I., and R. Sausen, 1994: On the global transport of nitrogen oxides from emissions of aircraft. In: Schumann and Wurzel (1994), 193-198.

Meijer, E. W., P. F. J. van Velthoven, W. M. F. Wauben, J. P. Beck, and G. J. M. Velders, 1997: The effects of the conversion of nitrogen oxides in aircraft exhaust plumes in global models. Geophys. Res. Lett. 24(23), 3013-3016.

Meijer, E. W., 2001: Modeling the impact of subsonic aviation on the composition of the atmosphere. Ph. D. Thesis, Tech. Univ. Eindhoven, The Netherlands, 108 pp.

Meilinger, S. K., B. Kärcher, R. von Kuhlmann, and T. Peter, 2001: On the impact of heterogeneous chemistry on ozone in the tropopause region. Geophys. Res. Lett. 28(3), 515-518.

Möllhoff, M., 1996: Modellierung der chemischen Umwandlung reaktiver Flugzeugabgase im Tropopausenbereich unter Berücksichtigung ihrer Dispersion. Diploma thesis, Institut für Geophysik und Meteorologie, Universität zu Köln, 110 pp.

Petry, H., J. Hendricks, M. Möllhoff, E. Lippert, A. Meier, A. Ebel, and R. Sausen, 1998: Chemical conversion of subsonic aircraft emissions in the dispersing plume: Calculation of effective emission indices. J. Geophys. Res. 103 (D5), 5759-5772.

Sausen, R., I. Isaksen, V. Grewe, D. Hauglustaine, D. S. Lee, G. Myhre, M. O. Köhler, G. Pitari, U. Schumann, F. Stordal, and C. Zerefos, 2005: Aviation radiative forcing in 2000. An update on IPCC (1999). Meteorol. Z. 14, 555–561.

Schumann, U., H. Schlager, F. Arnold, R. Baumann, P. Haschberger, and O. Klemm, 1998: Dilution of aircraft exhaust plumes at cruise altitudes. Atmos. Environ. 32, 3097-3103.

Uphoff, M., 2008: Parametrisierung flugzeuginduzierter Vermischung in einem mesoskaligen Modell (Parameterisation of aircraft-induced mixing in a mesoscale model). Diplomarbeit, Universität Hamburg, 144 pp. [In German]

ECHAM5 simulations with the $HO_2 + NO \rightarrow HNO_3$ reaction

K. Gottschaldt*, C. Voigt[1], B. Kärcher
Deutsches Zentrum für Luft- und Raumfahrt (DLR) - Institut für Physik der Atmosphäre, Oberpfaffenhofen, Germany
[1]also: Universität Mainz, Institut für Physik der Atmosphäre

Keywords: climate modelling, atmospheric chemistry, ozone, nitric acid

ABSTRACT: A HNO_3-forming channel of the HO_2 + NO reaction recently found in laboratory measurements (Butkovskaya et al., 2005, 2007) may significantly alter the concentration of HNO_3, NO_x, O_3 and other trace gases in the tropopause region. This region is also significantly affected by air traffic NO_x emissions. Cariolle et al. (2008) adopted a pressure- and temperature dependent parameterisation of the rate constant to assess the impact of the HO_2 + NO -> HNO_3 reaction on trace gas concentrations in a 2-D stratosphere-troposphere model, and a 3-D tropospheric chemical transport model. We implemented the parameterisation of Cariolle et al. (2008) into the 3-D stratosphere-troposphere chemistry-climate model ECHAM5 / MESSy. Here we present results of our test runs, in support of planned studies of the effects of aircraft emissions on atmospheric chemistry.

1 BACKGROUND

The concentration of ozone in the upper troposphere and lower stratosphere region (UTLS) is mainly controlled by the reactive NO_x and HO_x cycles (figure 1).

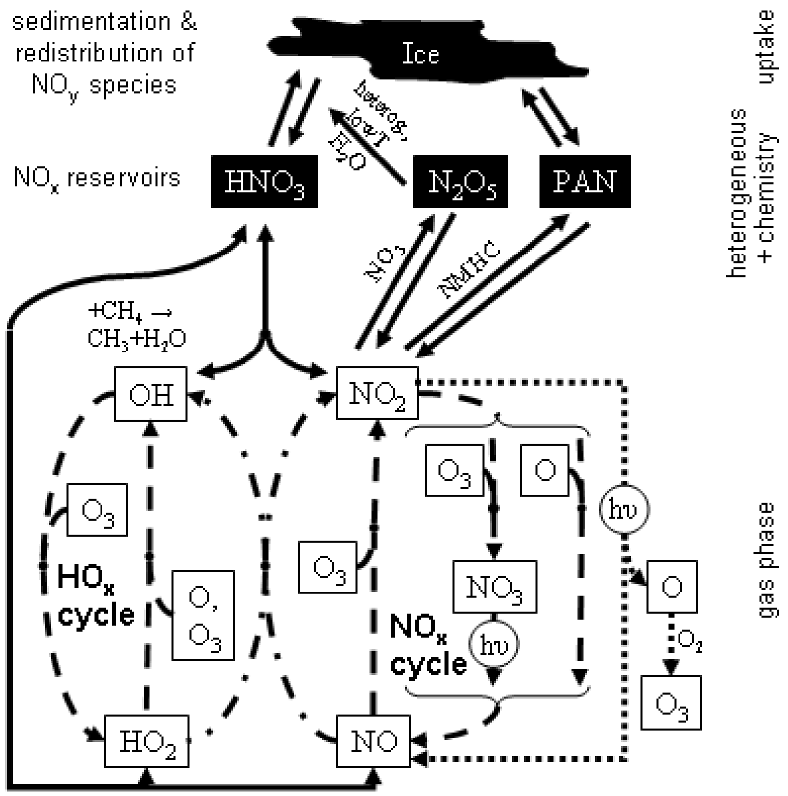

Figure 1. Major reactions in the UTLS involving ozone, methane NO_x, NO_y and HO_x. Solid lines represent reservoir reactions, dotted lines show reaction paths of ozone production, dashed paths indicate ozone destruction, and dash dot is neutral with respect to ozone.

* *Corresponding author:* Klaus Gottschaldt, Deutsches Zentrum für Luft- und Raumfahrt (DLR) - Institut für Physik der Atmosphäre, Oberpfaffenhofen, D-82234 Wessling, Germany. Email: klaus-dirk.gottschaldt@dlr.de

Aircraft NO_x emissions peak in the UTLS. Considering gas phase chemistry, the NO_x effect on ozone changes sign in the altitude range between about 12 and 18 km (Søvde et al., 2007). Below the tipping point, the ozone destructing NO_x cycle is bypassed via peroxy radicals. NO_x emissions lead to increased ozone production. Peroxy radicals and NO_2 photolysis are less important at higher altitudes. There aircraft NO_x emissions intensify the NO_x cyle, enhancing ozone destruction. NO_x may be removed from the system by heterogeneous reactions, but also by the recently discovered HNO_3-forming channel of the HO_2 + NO reaction (Butkovskaya et al., 2005, 2007):

$$k_1; \quad HO_2 + NO \rightarrow NO_2 + OH \tag{1}$$

$$k_2; \quad HO_2 + NO \rightarrow HNO_3 \tag{2}$$

with the rate constants k_1 and k_2.
The HO_2 + NO conversion has been assumed to have a temperature-dependent rate constant (Sander et al., 2003),

$$k_0 = k_1 + k_2 = 3.5 \cdot 10^{12} \cdot \exp\left(\frac{250}{T}\right) \tag{3}$$

with temperature T in [K]. In the following we study the effects of three different combinations of k_1 and k_2 on UTLS gas phase chemistry, extending the work of Cariolle et al. (2008).

2 BASE MODEL

We use the global chemistry-climate model ECHAM5 (Roeckner et al., 2003) / MESSy (Jöckel et al., 2006). Dynamics and chemistry are fully coupled. Our runs are based on the setup of Jöckel et al. (2006), but using MESSy version 1.6, with T42 / L90 resolution and the top layer centered at 0.01 hPa. Gas phase chemistry was calculated with the MECCA1 chemistry module (Sander et al., 2005), consistently from the surface to the stratosphere. However, the runs presented here were originally designed to find a parameterisation for correcting upper stratospheric chemistry in low resolution models. Therefore our chemical mechanism has full stratospheric complexity, but neglects the NMHC, sulfur, and halogen families in the troposphere. The initial conditions correspond to January 1978 and we evaluated twelve months, starting November 1978.
Figures 2a show the 12-month average of the zonal mean mixing ratios for HNO_3, NO_x and O_3, in the base model, run A. Reaction 1 is included with $k_1 = k_0$ (equation 3). The HNO_3-forming channel (reaction 2) is ignored here, i.e. $k_2 = 0$.

3 EFFECTS OF THE HO2 + NO → HNO3 REACTION

Simulation B differs to the base run just in k_1 and k_2:

$$k_2 = \frac{k_0 \cdot \beta}{1 + \beta} \tag{4}$$

$$k_1 = k_0 - k_2 \tag{5}$$

with pressure p [Pa] in

$$\beta(p,T) = 0.01 \cdot \left(\frac{530}{T} + p \cdot 4.8 \cdot 10^{-6} - 1.73\right). \tag{6}$$

Hence both reaction rates depend on temperature and pressure in this case. Equation 6 was proposed by Cariolle et al. (2008). It is based on an empirical fit to measurements and valid for dry conditions, in the range 93 - 800 hPa and 223 - 298 K. They noted deviations from equation 6 for temperatures above 298 K.
Figures 2b show the differences d between run B and the base model. The results are noisy, because both runs, A and B, were dynamic. They had all couplings between chemistry and meteorology switched on. Running the ECHAM model in a chemistry transport mode would have been better

suited for our sensitivity runs B and C, but this option was not available. Given the exploratory nature of this study, we believe the present approach is acceptable. Due to the different dynamics in both runs, a low background value in one model might coincidentally fall together with a high value in the other model. The biggest effects on HNO_3, NO_x and O_3 correlate with rather small background mixing ratios. To filter out some noise, and to avoid random division by numbers close to zero, we normalized all values *d* by the locally highest background value:

$$d = \frac{v_B - v_A}{\max(v_A, v_B)} \cdot 100\% \qquad (7)$$

v_A and v_B are the zonal mean mixing ratios of the same species, in the base run and model B, respectively. We get similar variations to the base model as Cariolle et al. (2008). They show results for March only. However, in another attempt to reduce noise, we evaluated 12 months instead of just March. Results for March display a similar pattern as the yearly mean, in our runs.

Inclusion of the HNO_3 forming channel results in a general HNO_3 increase, prompting an overall NO_x decrease. As expected, ozone correlates with NO_x variations below ≈12 km, while there is anticorrelation above ≈18 km.

Cariolle et al. (2008) applied equation 6 up to an altitude of 30 km, although it is only based on measurements for pressures corresponding to an altitude of about 15 km. Therefore we did not expect any problems for lower pressures and applied equation 6 up to 0.01 hPa (39 km). Similar to Cariolle et al. (2008), we get a locally pronounced HNO_3 increase about 15 km over the equator, followed by a region of smaller effects and another increase from 25 km upwards. However, in our model we note the biggest relative HNO_3 increase above 30 km. It remains unclear if this effect is real, an artefact due to the extrapolation of equation 6, or due to the very low background concentration in that altitude.

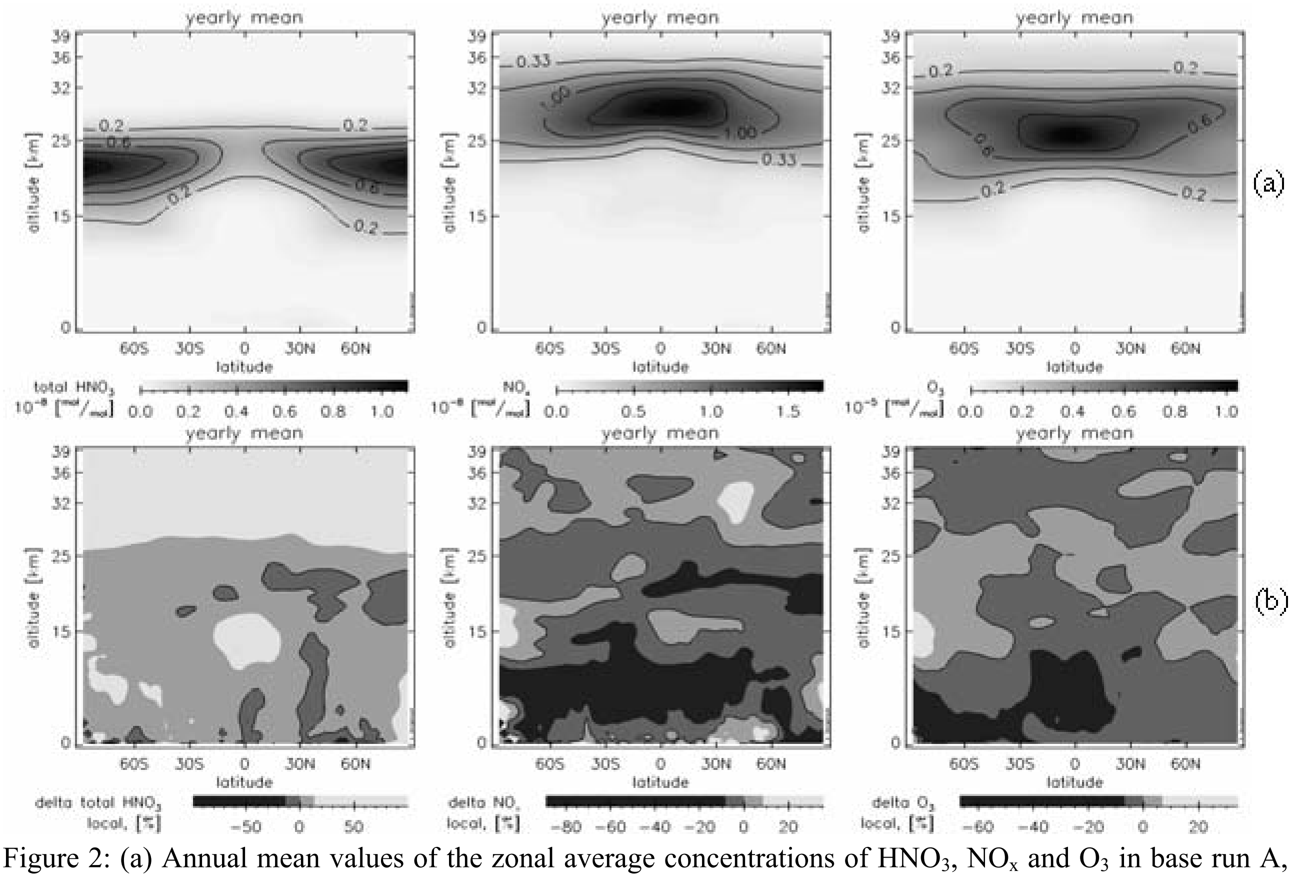

Figure 2: (a) Annual mean values of the zonal average concentrations of HNO_3, NO_x and O_3 in base run A, without $HO_2 + NO \rightarrow HNO_3$ reaction; (b) Run B: deviations from A after inclusion of the dry HNO_3 reaction

4 CONCLUSIONS

The HNO_3 forming channel of the HO_2 + NO reaction has the potential to alter UTLS chemistry significantly. Adding the dry HO_2 + NO → HNO_3 reaction to our model resulted in a general increase of HNO_3, a decrease of NO_x and related effects on ozone. The spatial pattern of variations confirms the results of Cariolle et al. (2008). However, it is not clear if the parameterisation used for the reaction rate is valid above 15 km. Measurements under stratospheric conditions are needed. At any rate, it is important to confirm the data set presented by Butkovskaya et al. (2005, 2007) by independent laboratory studies. A better noise reduction strategy and refined tropospheric chemistry in the model might be useful to study the impact of this reaction in more detail.

5 ACKNOWLEDGEMENTS

The authors thank Christoph Brühl, Georges Le Bras, Patrick Jöckel and the Messy-Team for their support.

REFERENCES

Butkovskaya, N.I., Kukui, A., Pouvesle, N., and G. Le Bras, 2005: Formation of nitric acid in the gas-phase HO_2+ NO reaction: Effects of temperature and water vapor. *J. Phys. Chem. A 109,* 6509–6520.

Butkovskaya, N.I., Kukui, A., and G. Le Bras, 2007: Study of the HNO_3 forming channel of the HO_2 + NO reaction as a function of pressure and temperature in the ranges 72 - 600 Torr and 223 - 323 K. *J. Phys. Chem. A 111,* 9047-9053.

Cariolle, D., Evans, M.J., Chipperfield, M.P., Butkovskaya, N., Kukui, A., and G. Le Bras, 2008: Impact of the new HNO_3-forming channel of the HO_2 + NO reaction on tropospheric HNO_3, NO_x, HO_x and ozone. *Atmos. Chem. Phys. 8,* 4061-4068.

Jöckel, P., Tost, H., Pozzer, A., Brühl, C., Buchholz, J., Ganzeveld, L., Hoor, P., Kerkweg, A., Lawrence, M.G., Sander, R., Steil, B., Stiller, G., Tanarhte, M., Taraborrelli, D., van Aardenne, J., and J. Lelieveld, 2006: The atmospheric chemistry general circulation model ECHAM5/MESSy1: consistent simulation of ozone from the surface to the mesosphere. *Atmos. Chem. Phys. 6,* 5067–5104.

Roeckner, E., Bäuml, G., Bonaventura, L., Brokopf, R., Esch, M., Giorgetta, M., Hagemann, S., Kirchner, I., Kornblueh, L., Manzini, E., Rhodin, A., Schlese, U., Schulzweida, U., and A. Tompkins, 2003: *The atmospheric general circulation model ECHAM5.* Technical Report No. 349, Max-Planck-Institut für Meteorologie, Hamburg, Germany, ISSN 0937-1060, 127 pp.

Sander, R., Kerkweg, A., Jöckel, P., and J. Lelieveld, 2005: Technical note: The new comprehensive atmospheric chemistry module MECCA. *Atmos. Chem. Phys. 5,* 445–450.

Sander, S.P., Finlayson-Pitts, B.J., Friedl, R.R., Golden, D.M., Huie, R.E., Kolb, C.E., Kurylo, M.J., Molina, M.J., Moortgat, G.K., Orkin, V.L., and A.R. Ravishankara, 2003: *Chemical Kinetics and Photochemical Data for Use in Atmospheric Studies, Evaluation Number 14*. JPL Publication 02-25, Jet Propulsion Laboratory, Pasadena, CA.

Søvde, O.A., Gauss, M., Isaksen, I.S.A., Pitari, G., and C. Marizy, 2007: Aircraft pollution – a futuristic view. *Atmos. Chem. Phys. 7*, 3621-3632.

Long-term 3D Simulation of Aviation Impact on Ozone Precursor Chemistry using MOZART-2

J. Hurley*,
Centre for Air Transport and the Environment, Manchester Metropolitan University, Manchester, United Kingdom

Keywords: Simulation, Aviation, Ozone, Chemistry, MOZART-2

ABSTRACT: Emission of aviation carbon dioxide (CO_2) and nitrogen oxides (NO_x) affects atmospheric composition through a complicated system of chemical reactions associated with ozone (O_3) and its precursors. The Model for Ozone and Related Chemical Tracers MOZART (version 2) is a three-dimensional global chemical transport model which considers 63 species as involved in some 170 reactions, with a scheme for ozone, nitrogen oxides and hydrocarbons – and hence is well-suited for quantifying the impact of aviation emissions upon atmospheric chemistry. In this preliminary study, a multi-year MOZART simulation is presented to analyse the behaviour of the aviation emission impact on important chemical fields such as O_3, hydroxide (OH), methane (CH_4), carbon monoxide (CO) and NO_x over a period of 10 years in such a chemical transport model, using QUANTIFY A1 emissions for 2000.

1 INTRODUCTION

1.1 *Ozone Precursor Chemistry Pertinent to Aviation*

Anything entering the global atmospheric system affects it in some way or another, however benign it may seem. In terms of chemical or aerosol emission, such as resulting from aircraft activity in the upper troposphere or lower stratosphere, it is obvious that adding species to a naturally clean region of the atmosphere will result in notable changes. These effects are predominantly expected to occur in the region of the emission perturbation – however due to atmospheric dynamics and circulation, may eventually affect large portions of the global atmosphere. In the specific case of aviation, the ozone family of species is most affected. It is thus important to quantify the effect that emission of aviation emissions on the atmosphere, taking ozone precursors as indicators of the perturbation.

From a first order, the largest deviations are expected in the regions in which aircraft activity is a maximum (see Section 1.3). This corresponds to the 1000 – 2000 Pa range (which converts to altitudes around 10 km) as there is a maximum of aircraft activity in that altitude range. Furthermore, the deviations should be focussed in the Northern mid-latitudes – again, in accordance with the large proportion of air traffic occurring in this region – and dominant features such as the North Atlantic flight corridor and point sources such as busy international hubs are expected to show prominent deviations.

As well, there are expected trends in the manner in which atmospheric trace species respond to emission of CO and NO_x from aircraft. The short-term response is linked to the set of reactions:

$$\begin{aligned} &H_2O + NO \rightarrow OH + NO_2 \\ &N_2O + h\upsilon \rightarrow NO + O \\ &O_2 + O \rightarrow O_3 \end{aligned} \quad (1)$$

* Corresponding author: Jane Hurley, Manchester Metropolitan University,Department of Environmental and Geographical Science, John Dalton Building, Chester Street, Manchester M1 5GD, United Kingdom. Email: j.hurley@mmu.ac.uk

whilst the long-term response is determined by the interplay between:

$$O_3 + HO_2 \rightarrow OH + 2O_2$$
$$CH_4 + OH + O_2 \rightarrow CH_3O_2 + H_2O \quad (2)$$
$$CO + OH + O_2 \rightarrow CO_2 + HO_2.$$

In the short-term (less than approximately 2 months), there is an increase in NO_x, O_3 and OH and a decrease in CH_4. Over the long-term, the production of O_3 is overcome and there is a persistent destruction of O_3. There persists a long-term destruction of CH_4 – however the long-term concentration of OH is dependent upon the balance between the O_3 and CH_4 destruction.

1.2 *Overview of MOZART-2*

The Model for Ozone **a**nd Related Chemical Tracers (MOZART, Horowitz, 2003) is a global chemical transport model which is driven by meteorological fields (generated either by a climate model or by measurement fields) to simulate the chemical composition of the troposphere and lower stratosphere (in version 2, used here) in T63LR resolution (roughly 2.8° x 2.8° x 19 levels vertically extending to 1000 Pa).

The second version of MOZART, MOZART-2, considers 63 species as involved in some 170 reactions, with a scheme for ozone, nitrogen oxides and hydrocarbons –and is solved with a 20 minute time-step. It considers emissions such as surface emissions from fossil-fuel combustion, biomass burning, biogenic processes involving vegetation and soils, exchanges with oceans, aircraft emissions and production of NO_x from lightning. It also takes into account dynamical processes such as advective and convective transport, boundary layer mixing as well as phenomena such as cloudiness and precipitation, and allows for wet and dry deposition of chemical species.

MOZART-2 is not fully coupled – rather it is "one-way" coupled, such that atmospheric dynamics affect atmospheric chemistry but that the chemistry does not affect the dynamics. This enables study of specific chemical processes and attribution of changes in atmospheric constituents to changes in particular species – and hence is a good candidate for use in sensitivity studies.

1.3 *Emissions Data*

In order to isolate the impact of aviation emissions upon the atmospheric chemical system, it is important to differentiate between natural and anthropogenic (exclusive of aircraft) emissions, and those deriving from aviation.

Background emissions are taken as those provided default to MOZART-2, as detailed in Friedl (1997). The QUANTIFY A1 inventory (B. Owen, pers. comm.) compiled at the Centre for Air Transport and the Environment (CATE) has been used to detail the emissions from aviation into the atmospheric system. The CATE QUANTIFY A1 inventory considers the 2000 base-case (using IEA 2000 fuel- use statistics), as well as a range of future scenarios. It catalogues the distance flown, total fuel used, and mass of CO_2, NO_x, and black carbon emitted per year in gridboxes of 1° x 1° x 610 m (as flight levels). MOZART-2 requires NO_x and CO as input for aviation emissions – and as CO emissions are not catalogued in the QUANTIFY dataset, an emission index of 0.3 is used to scale the fuel emissions to estimate the emitted CO (B. Owen, pers. comm.). Figure 1 shows the average vertically-integrated global distribution of aviation emissions as well as the average latitude-altitude distribution of aviation emissions for CO and NO_x.

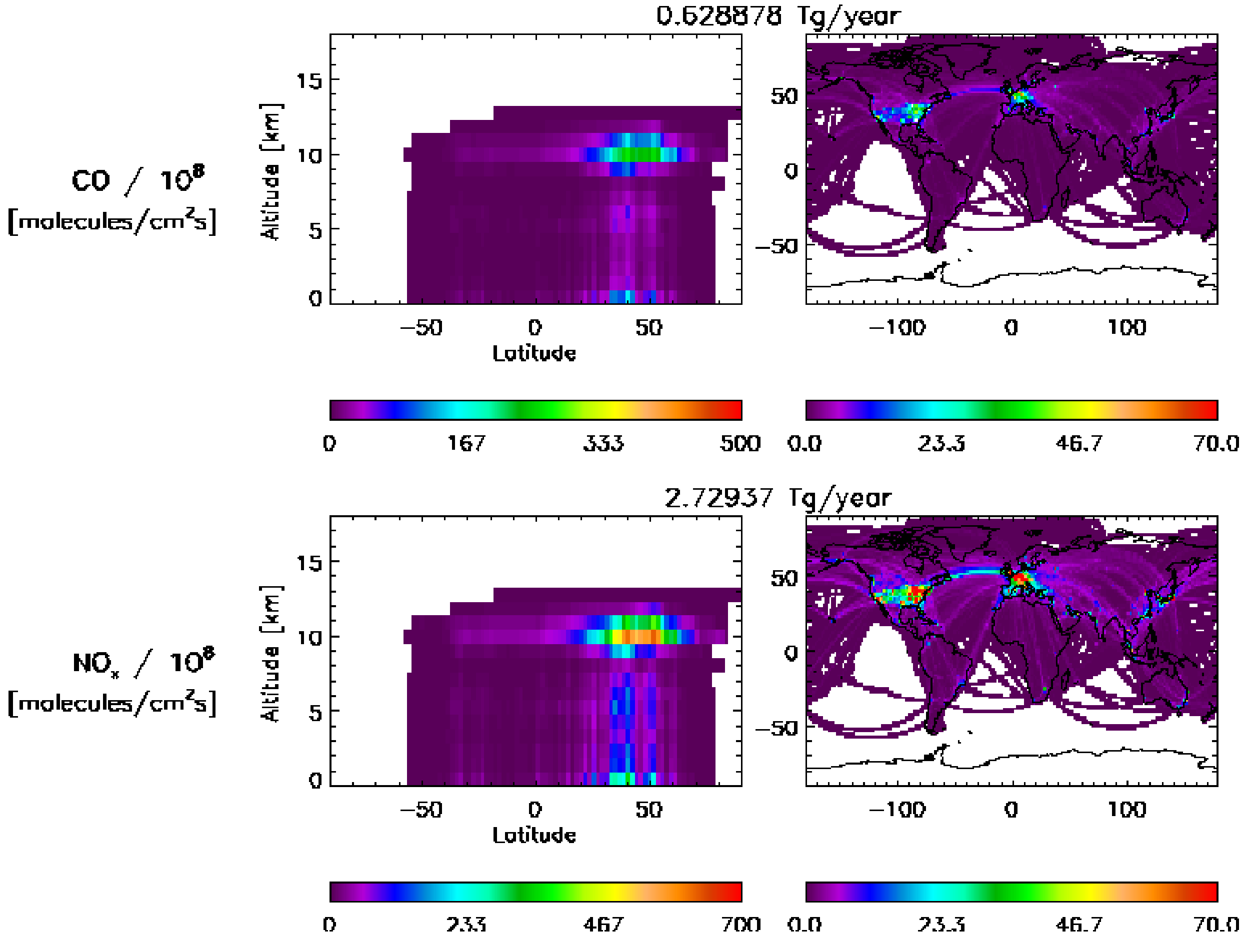

Figure 1. Aircraft emissions of CO (top panels) and NO_x (bottom panels) for CATE QUANTIFY inventory, averaged on both a latitude/altitude (left panels) and latitude/longitude (right panels) grid.

1.4 *Simulation Approach*

European Centre for Medium-Range Weather Forecasts (ECMWF, 2005) products for 2003 have been used for the dynamical and meteorological fields for all simulations, regardless of simulation year, so that the evolution of changes in chemistry due to changing aircraft emissions cannot be attributed to differences in synoptics specific to a particular year.

Difference between simulations with and without aviation emissions is used to isolate the impact of aviation emissions for 'present-day' conditions (2000). Thus, having run MOZART-2 with and without aircraft emissions (labelled 'a' for 'with aircraft' and 'na' for 'with no aircraft', the effect upon global chemistry and composition is studied, using the relative difference between the volume mixing ratios (vmr) of each chemical species studied (O_3, OH, nitrogen dioxide NO_2, CO and CH_4) for the simulations run with about without aircraft emissions is defined as

$$vmr_{rd}(x,y,z) = \frac{vmr_{na}(x,y,z) - vmr_{a}(x,y,z)}{vmr_{na}(x,y,z)} \times 100\% \qquad (3)$$

where vmr_{rd} is the relative difference in vmr of the 'no-aircraft' (vmr_{na}) and 'aircraft' (vmr_a) cases, for longitude x, latitude y and altitude/pressure/level z. Whilst MOZART-2 outputs on hybrid-sigma pressure levels, all results here are presented on pressure levels, as they are more intuitively associable with altitudes – and because the aircraft emissions are given on altitude grids.

However, CH_4 is long-lived, taking upwards to 80 years to reach equilibrium in the atmosphere – a timeframe which is prohibitively out of range from a computational perspective. Hence, the CH_4 output by MOZART-2 after a typical single/several year run is not near to being in steady-state – which is why the unprocessed impact on CH_4 will be much less than expected. According to Fuglestvedt (1998), for a perturbed state from a simulation which is in chemical equilibrium, the perturbed steady-state concentration of CH_4, $[CH_4]_{ss}$, can be estimated using the concentration of

CH4 from the equilibrated simulation, $[CH4]_{ref}$, and the lifetimes τ for the perturbed and equilibrated simulations:

$$[CH_4]_{ss} = [CH_4]_{ref}\left(1 + 1.4\frac{\tau_{per} - \tau_{ref}}{\tau_{ref}}\right) \quad (4)$$

This correction is applied to CH_4 fields output by MOZART-2 to extrapolate to the steady-state impact from the aviation perturbation.
In the current study, MOZART-2 is "spun-up" for a period of one year, and consequently run for a period of 10 years.

2 RESULTS

Timelines of the overall global burden as well as of the aircraft impact of each O_3 precursor are shown in Figure 2. The O_3 impact of aviation is dying away, as expected in the short-term, whilst the impact on all precursors appears to still be evolving and increasing – undoubtedly due to the longer CH_4 response.

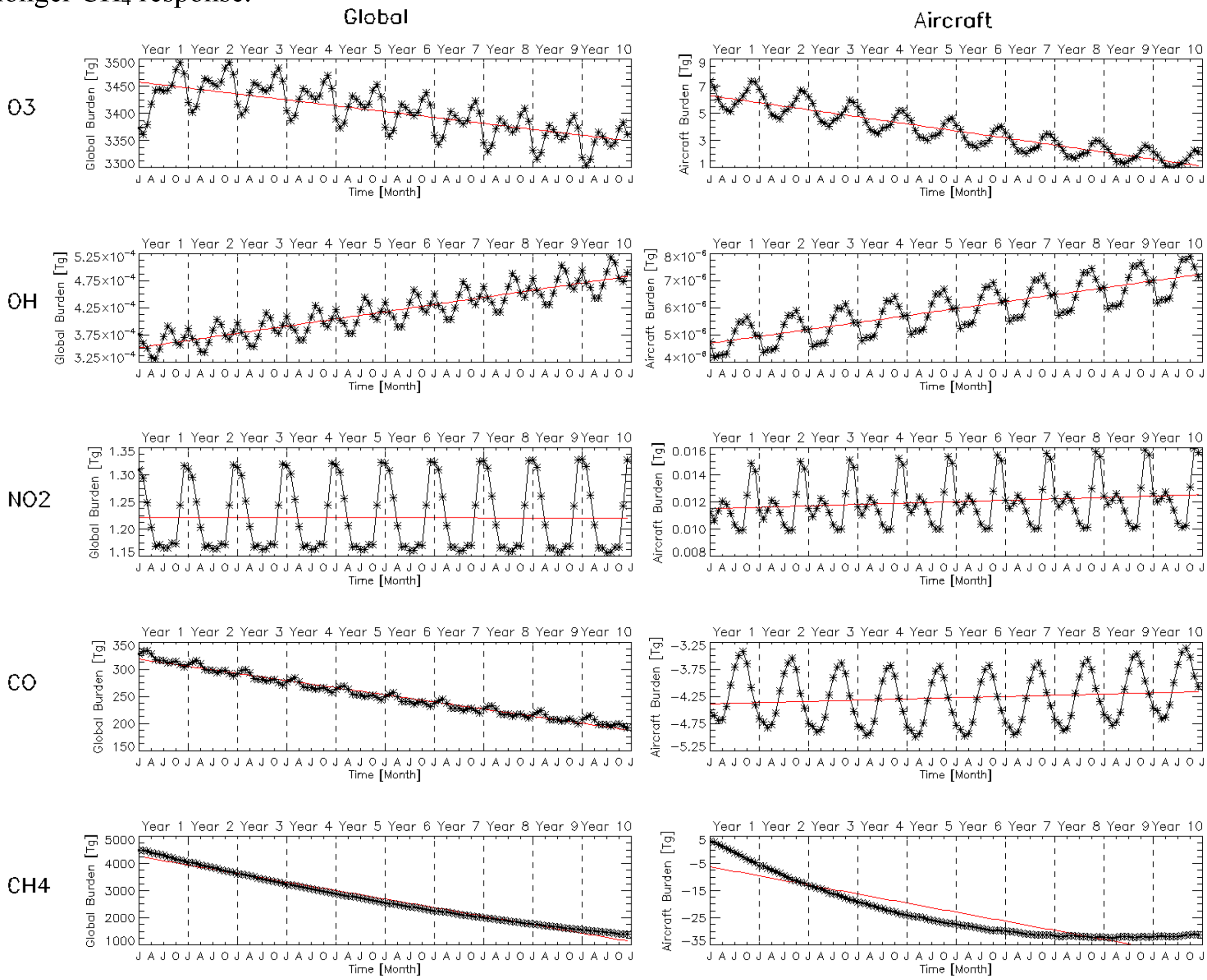

Figure 2. Global total burden (left panels) and burden attributable to aviation impact (right panels) as a function of simulated time.

Figure 3 shows the time evolution of the annual averages on a latitude/pressure grid of the aviation impact in terms of the relative difference from the base 'no-aircraft' state, for each species. In general, the changes in concentration due to inclusion of aviation emissions simulated by MOZART-2 agree with those expected from previous studies – quantifying values are tabulated in Table 1.

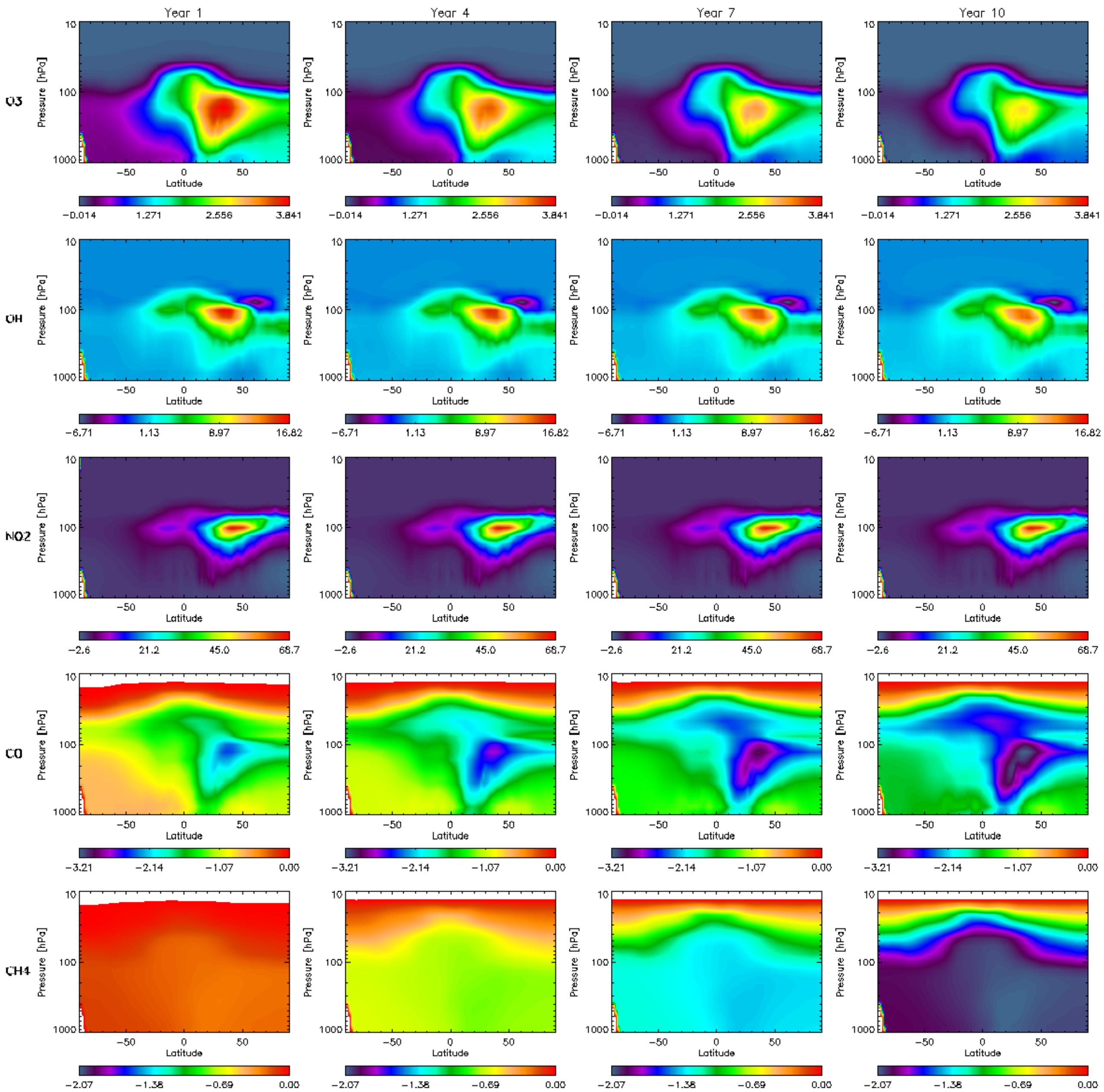

Figure 3. Relative differences in concentrations for O_3 precursor species (O_3 top, OH second, NO_2, third, CO fourth, and CH_4 bottom panels) due to the perturbation caused by aviation emissions.

Table 1. Volume mixing ratios for O3 precursors as well as relative aviation impact, as expected from literature and outputted by MOZART-2. (eg. Brasseur et al., 1996; Kinnison et al., 2007; MIPAS, 2009)

Species	Absolute Volume Mixing Ratio Without Aviation		Aviation Impact, Change [%] Maximum / Mean	
	Expected	MOZART	Expected	MOZART
O_3	0 – 8 ppm	0 – 15 ppm	4% / 1%	4% / 0.8%
OH	0.3 – 1.5 ppt	0 – 13 ppt	20% / 5%	17% / 0%
NO_2	0 – 10 ppb	0 – 8 ppb	30% / 10%	65% / 0%
CO	30 – 200 ppb	14 – 202 ppb	? / ?	-3% / -1%
CH_4 (steady-state)	0 – 3 ppm	0.3 – 1.6 ppm	? / -1%	-2% / -2%

As the CH_4 calculated by MOZART-2 is far from the final steady-state value, because the system is not in equilibrium for CH_4, Fuglestvedt's approximation has been applied for each year – and the steady-state concentration of CH_4 estimated, with and without aircraft, as well as the change in CH_4 due to aviation emissions in absolute volume-mixing-ratio and in relative difference, as shown in Figure 4.The steady-state CH_4 response appears to marginally grow in time.

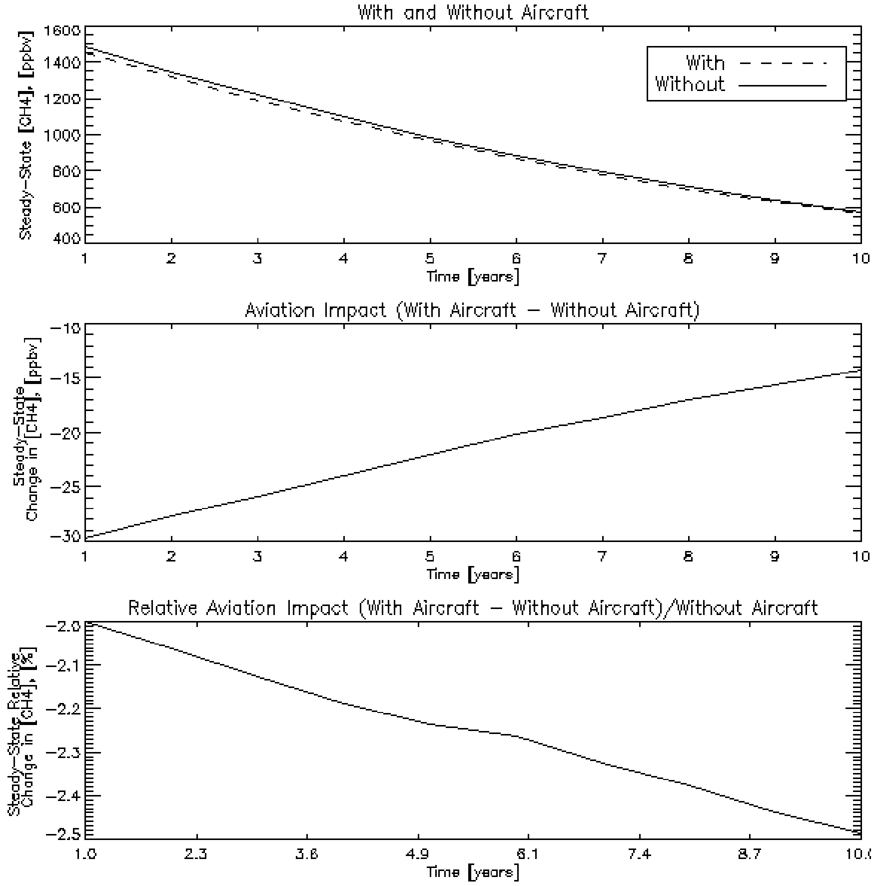

Figure 4. Estimates of steady-state concentration of CH4 perturbation using Fuglesvedt (1998).

3 CONCLUSIONS

A long-term decade-long simulation of the impact of aviation emissions tabulated for 2000 on the chemistry of O_3 and its precursors has been carried out using the three-dimensional chemical transport model MOZART-2. As most O_3 precursors are short-lived, the difference between simulations with and without emissions seems sufficient to estimate the impact of aviation emissions; however CH_4, a long-lived species, must have a correction applied in order to quantify the steady-state impact. The relative changes in concentration predicted by MOZART-2 agree well with those determined by previous studies.

REFERENCES

Brasseur, G., J. Müller, and C. Granier, 1996: Atmospheric impact of NOx emissions by subsonic aircraft: A three-dimensional study, J. Geophys. Rev., 101, pp.1423 – 1428.

ECMWF website, accessed 25 February 2009: http://www.ecmwf.int/, 2005.

Friedl, R. (ed.), 1997: Atmospheric Effects of Subsonic Aircraft-Interim Assessment Report of the Advanced Subsonic Technology Program, NASA Reference Publication 1400, 143 pp.

Fuglestvedt, J., T. Berntsen, I. Isaksen, H. Mao, X. Liang, and W. Wang, 1999: Climatic forcing of nitrogen oxides through changes in tropospheric ozone and methane; global 3D model studies, Atmos. Env., 33, pp. 961 – 977, 1998.

Horowitz, L., S. Walters, D. Mauzerall, L. Emmons, P. Rasch, C. Granier, X. Tie, J. Lamarque, M. Schultz, and G. Tyndall, 2003: A global simulation of tropospheric ozone and related tracers: Description and evaluation of MOZART, version 2.J. Geophys. Res., 108, 4784, doi: 10.1029/2002JD002853.

Kinnison, D., G. Brasseur, S. Walters, R. Garcia, D. Marsh, F. Sassi, V. Harvey, C. Randall, L. Emmons, J. Lamarque, P. Hess, J. Orlando, X. Tie, W. Randel, L. Pan, A. Gettelman, C. Granier, T. Diehl, U. Niemeier, and A. Simmons, 2007: Sensitivity of chemical tracers to meteorological parameters in the MOZART-3 chemical transport model, J. Geophys. Rev., 112, D20302, doi:10.1029/2006JD007879.

MIPAS webpage at University of Oxford, accessed 17 July 2009: http://www.atm.ox.ac.uk/group/mipas/L2OXF/index.html, 2009.

QUANTIFY model evaluation of global chemistry models: carbon monoxide

C. Schnadt Poberaj[*9], J. Staehelin
Institute for Atmospheric and Climate Science, ETH Zürich, Switzerland

R. Bintania, P. van Velthoven
Royal Netherlands Meteorological Institute (KNMI), Atmospheric Composition Research, De Bilt, the Netherlands

O. Dessens
Centre for Atmospheric Science, Department of Chemistry, University of Cambridge, United Kingdom

M. Gauss, I.S.A. Isaksen
University of Oslo, Department of Geosciences, Oslo, Norway

V. Grewe, P. Jöckel
DLR-Institut für Physik der Atmosphäre, Oberpfaffenhofen, Germany

P. Hoor
Institut für Physik der Atmosphäre, Johannes Gutenberg-Universität Mainz, Mainz, Germany

B. Koffi, D. Hauglustaine
Laboratoire des Sciences du Climat et de l'Environment, Gif-sur-Yvette, France

D. Olivié
Centre National de Recherches Météorologiques (CNRM), Toulouse, France

Keywords: model evaluation, global chemistry models, carbon monoxide, emissions

ABSTRACT: In the EU Integrated project QUANTIFY, atmospheric chemistry models (ACMs) are one of the major tools to improve the understanding of key processes relevant for the effects of different transportation modes, and their representation in global models. The performance of the ACMs has been tested through comparisons with the ETH model evaluation global database for the upper troposphere and lower stratosphere. Data from measurement campaigns, ozone soundings, and surface data have been processed to support an easy and direct comparison with model output. Since model evaluation focuses on the year 2003, observational data to compare model data with are the SPURT campaign and the commercial aircraft program MOZAIC. The model evaluation indicates a particular problem in the simulation of carbon monoxide. If QUANTIFY emissions inventories are used, models significantly underestimate its tropospheric abundance at northern hemispheric middle latitudes and subtropical latitudes. Potential causes will be discussed.

1 INTRODUCTION

Global atmospheric chemistry models (ACMs), i.e. chemistry transport models (CTMs) and chemistry-climate models (CCMs) have become standard tools to study tropospheric and stratospheric photochemistry and the impact of different emission sources onto the atmospheric composition including scenarios for future emission changes. Studies based on such models were a central element in scientific assessments of the impact of present and future air traffic emissions (Brasseur et al., 1998; Penner et al., 1999; NASA, 1999). In the EU FP6 Integrated Project (IP) QUANTIFY (Quantifying the Climate Effect of Global and European Transport Systems) ACMs are used to improve the understanding of the relative effects of different transportation modes on the atmospheric com-

[*] *Corresponding author:* Christina Schnadt Poberaj, Institute for Atmospheric and Climate Science, Universitaetstrasse 16, ETH Zurich, CHN, 8092 Zurich, Switzerland. Email: christina.schnadt@env.ethz.ch

position, and their representation in global models. For instance, the impact of present-day traffic emissions on atmospheric ozone and the hydroxyl radical (OH) was evaluated by Hoor et al. (2009). To estimate the reliability of the models and hence of the studies investigating the impact of traffic emissions, it is highly relevant to evaluate how well the models reproduce available observations. A first comprehensive model evaluation of ACMs operated by different groups in Europe was carried out by Brunner et al. (2003; 2005) in the framework of the EU project TRADEOFF. Brunner et al. (2003; 2005) compared model results with trace gas observations from several aircraft campaigns for the period 1995-1998. The present study uses updated versions of the models applied in Brunner et al. (2003; 2005). This paper focuses on the simulation of carbon monoxide (CO), one of the major atmospheric pollutants in densely populated areas, chiefly from exhaust of combustion engines by traffic, but also by incomplete burning of other fuels in industry. In the free troposphere, it has an indirect radiative forcing effect by elevating concentrations of tropospheric ozone through CO oxidation. Model results are compared to data from the commercial aircraft program MOZAIC (Marenco et al., 1998), as well as to aircraft campaign data. The next section summarises the main model characteristics, the boundary conditions used, and the methodology. Results of the model evaluation are shown in Section 3. Conclusions are presented in Section 4.

2 MODELS, DATA, AND METHODOLOGY

Within QUANTIFY model evaluation results from six models were compared with observational data. Four models are CTMs using prescribed operational ECMWF data to simulate meteorological conditions (TM4, p-TOMCAT, OsloCTM2, and MOCAGE) and two are CCMs (LMDzINCA and ECHAM5/MESSy), which were nudged toward operational ECWMF fields.

An overview of the main model characteristics is given in Hoor et al., 2009 (their Table 4), and in Table 1 for MOCAGE and ECHAM5/MESSy. The model setups are described in detail in Hoor et al. (2009) for TM4, p-TOMCAT, OsloCTM2, and LMDzINCA, in Teyssèdre et al. (2007) for MOCAGE, and in Jöckel et al. (2006) for ECHAM5/MESSy.

To force the models toward a realistic atmospheric state, emissions from different source categories were considered in the QUANTIFY numerical simulations. These are described in detail in Hoor et al. (2009). Emissions for the three transport sectors road, shipping, and air traffic were considered. The road traffic emissions inventory was developed within the QUANTIFY project. Except for a sensitivity simulation by OsloCTM2 (which used emissions from the POET project), the emissions used in this study are based on a draft version (Borken and Steller, 2006) (QUANTIFY preliminary, see Table 2 for CO emissions). An overview of CO emissions considered in the QUANTIFY

Table 1: Main characteristics of ECHAM5/MESSY and MOCAGE.

Model	MOCAGE	ECHAM5/MESSy
Operated	CNRM	MPICHEM
Model type	CTM	CCM (nudged)
Meteorology	ECMWF OD	ECMWF OD
Hor. resolution	T21	T42
Levels	60	90
Model top (hPa)	0.07	0.01
Transport scheme	Williamson & Rasch	Lin & Rood
Convection	Bechtold et al. (2001)	Tiedke-Nordeng
Lightning	Climatology	Price and Rind + Grewe
Transp. species	65	82
Total species	82	108
Gas phase reactions	186 + 47	178 + 57
Het. reactions	9	10 (PSC) + 26 (wet-phase)
Stratosph. chemistry	yes	yes
NMHC chemistry	yes	yes
Lightning NO_x (TgN/yr)	5	5

Table 2. CO emissions used in the QUANTIFY model simulations and comparison with TRADEOFF emissions (Brunner et al., 2003) (in Tg CO/yr). (*) Compare number in Hoor et al. (2009), their Table 1.

Species	Emission source	TRADEOFF	QUANTIFY preliminary	QUANTIFY final	OSLO POET
CO					
	Road traffic		73	110	196
	Ships		1.3	1.3	0.1
	Air traffic		1.1	1.1	
	Other anthropogenic		108	108	114
	Domestic burning (DB)		237	237	237
	Biomass burning (BB)	700	508	508	309
	Total anthr. fossil fuel (anthr.+road+ships+air)		183	220	310
	Total anthr. fossil fuel + DB	650	420	457	547
	Vegetation + soil	200	65*	65*	178
	Total	1550	993	1030	1034

simulations is given in Table 2.

Model output was generated and analysed with respect to trace gas observational data using point-by-point output, i.e. at each simulation time step, the instantaneous tracer fields were linearly interpolated to the positions of coinciding observations (Brunner et al., 2003; 2005). This method allows for a very close comparison with observations and fully accounts for the specific meteorological conditions of the measurements. By each modelling group the years 2002 and 2003 were simulated. 2002 was taken as spin-up, the year 2003 provided the base year for comparison with observations and sensitivity simulations (Hoor et al., 2009).

Model results were compared to data from the commercial aircraft program MOZAIC (Marenco et al., 1998), as well as to data from the SPURT (German: SPURenstofftransport in der Tropopausenregion) campaign (Engel et al., 2006). From MOZAIC, the one-minute averages of the CO measurements were evaluated. The 2003 SPURT campaigns took place in February, April, and July 2003 over Europe (Engel et al., 2006; their Fig. 4). Besides CO, ERA40 potential vorticity (PV) interpolated onto SPURT coordinates was used to distinguish between tropospheric and stratospheric air. The SPURT data were time averaged to yield one minute averages.

3 EVALUATION OF MODEL PERFORMANCE

Average model biases $(mean_{model}-mean_{obs})/mean_{obs}*100\%$ and root-mean-square (RMS) differences E of point-to-point model results and measurements are shown in Table 3 for the February 2003 SPURT campaign for the lowermost stratosphere (LMS, PV > 2 PVU) and the upper troposphere (UT, p < 500 hPa and PV < 2 PVU). Additional information on model performance can be summarised in a Taylor diagram (Taylor, 2001; Brunner et al., 2003): the correlation coefficient R, the centred pattern RMS difference E′ between a test vector f (model) and a reference vector r (observations), and the ratio of the standard deviations (σ_f /σ_r) of the two vectors are all indicated by a single point in a two-dimensional plot. For example, in Fig. 1a, the test point by MOCAGE (MO) refers to a correlation coefficient R=0.87, a normalised standard deviation σ_f/σ_r=0.95 (smaller modelled than observed σ), relatively large centred RMS difference (distance between reference and test point, only qualitative statement possible), and a skill score of > 0.9 (parabolic line of constant skill). For more details on the underlying algebra and relationships between statistical quantities see Taylor (2001) and Brunner et al. (2003) for the used definition of the skill score.

Upper tropospheric CO is underestimated by most models in all campaign months (≈-5% to -50%) except for OsloCTM2 (POET), for which a positive deviation of 10% to ≈35% is found. At higher altitudes in the LMS, negative biases are either significantly reduced or they turn to positive deviations. OsloCTM2, which exhibits positive biases in the UT, shows increased positive deviations from observations in the LMS. It could be suspected that the relatively low CO emissions from road traffic used in the QUANTIFY preliminary simulations (Table 2) might be responsible for the negative bias of most models. However, the negative deviations are not reduced or

Table 3: Mean model biases of CO (in %) for the 2003 SPURT campaigns for the lowermost stratosphere (PV > 2 PVU) (upper part) and the middle to upper troposphere (p < 500 hPa and PV < 2 PVU). Grey shading indicates negative deviation of a model mean from the respective observational value.

Model/Variable	February	April	July
	Lowermost stratosphere (LMS)		
OsloCTM2 (POET)	83±47	61±51	30±52
OsloCTM2	24±29	18±37	3±39
TM4	-13±21	-7±22	-22±27
p-TOMCAT	-27±19	-30±25	-44±23
MOCAGE	-13±26	32±58	-17±24
LMDzINCA	27±39	19±43	-3±38
ECHAM5/MESSy	-1±20	-4±25	-25±25
	Upper troposphere (UT)		
OsloCTM2 (POET)	35±55	37±59	10±54
OsloCTM2	-7±37	0±43	-11±41
TM4	-29±20	-17±30	-34±28
p-TOMCAT	-40±14	-43±23	-52±22
MOCAGE	-26±13	28±61	-19±30
LMDzINCA	-12±37	-5±50	-22±34
ECHAM5/MESSy	-18±27	-10±29	-33±28

eliminated when using QUANTIFY final road emissions, which are ≈50% higher than the preliminary emissions (Fig. 1b, compare OsloCTM2 simulations PRELIM and FINAL). Hence, the different performance of OsloCTM2 using POET emissions (Table 3, Fig. 1b) can probably not be (fully) explained by the higher road traffic CO emissions. Possibly, emissions of non-methane volatile organic compounds (NMVOCs), which are an additional non-negligible source of CO (IPCC, 2001), may play a role: in the POET emissions inventory these are known to be significantly higher over polluted regions than in other inventories. The altitude dependency of biases is largely reflected by MOZAIC profiles: as presented for Frankfurt, Germany, relative differences show a positive slope with altitude (Fig. 1b). This effect might be connected to an insufficient vertical resolution of the models to resolve the vertical CO gradient across the tropopause.

Using MOZAIC cruise level data, which are mostly representative of the LMS, similar biases as over Europe were identified on the hemispheric scale in all seasons (Fig. 1a for DJF, other seasons not shown). Note that the geographical bias patterns are not homogeneous for most models,

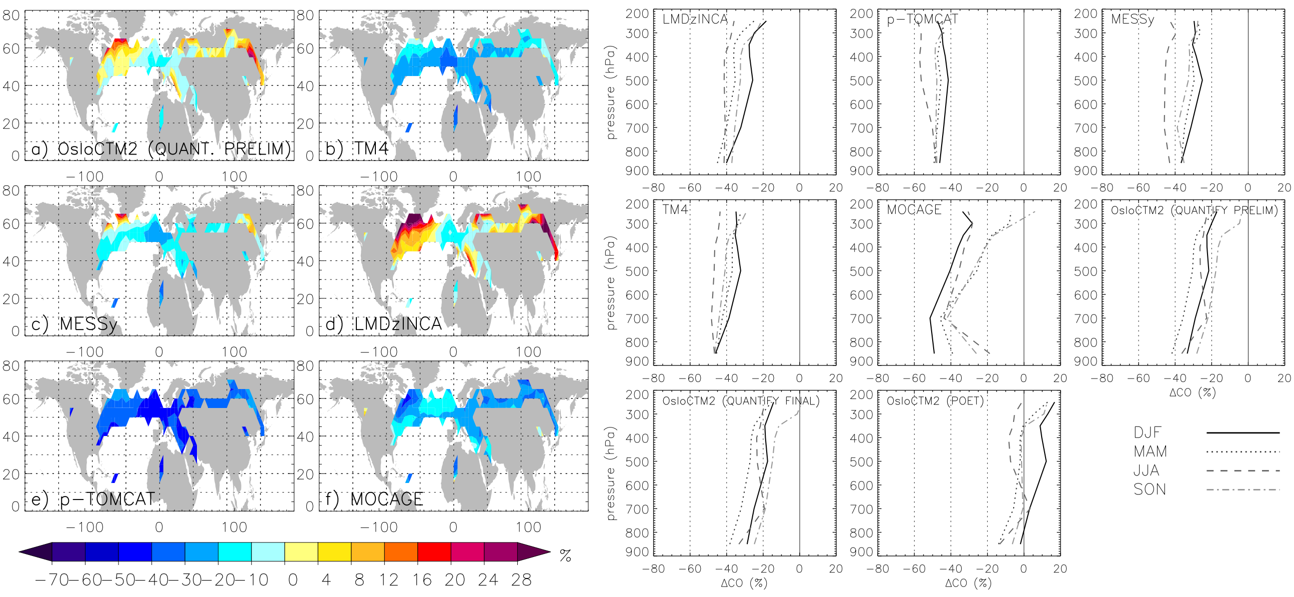

a) b)

Figure 1: Mean model biases for 2003 MOZAIC data (model-MOZAIC) (in %). a) Horizontal distribution from cruise level data at 300 hPa – 170 hPa, DJF 2003, biases only plotted if at least 20 measurements available in 5°x5° grid boxes; b) vertical profiles for Frankfurt, Germany, for DJF (black solid line), MAM (dark grey dotted line), JJA (grey dashed line), and SON (light grey dash-dotted line).

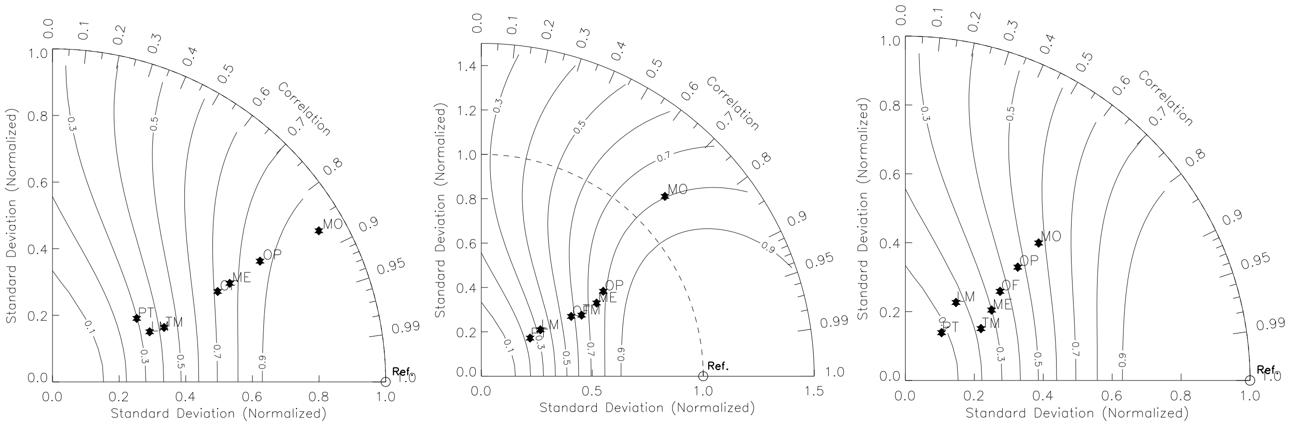

a) b) c)

Figure 2: Taylor diagrams of the comparison between observed and modelled CO for the SPURT campaigns 2003. a) February, b) April, and c) July 2003. Letters denote models: OP (OsloCTM2 with POET emissions), OF (OsloCTM2 with preliminary QUANTIFY emissions), TM (TM4), PT (p-TOMCAT), ME (ECHAM5/MESSy), MO (MOCAGE), and LM (LMDzINCA).

but show maximum negative deviation over Europe and smaller negative or even positive biases over Eastern USA and Siberia. This is due to regional features in the observed distribution, namely a CO maximum over Europe and relatively low mixing ratios over northern America and East Siberia (not shown), which are not fully captured by the models.

CO has a sufficiently large photochemical lifetime of 1-3 months in the troposphere (IPCC, 2001) to be transported on the hemispheric scale (e.g., Stohl et al., 2002). Thus, not surprisingly, the Taylor diagrams reveal high correlation coefficients in winter and spring 2003 ($0.8 \leq R \leq 0.9$) (Fig. 2a and b). In July, only somewhat smaller correlations ($0.5 < R \leq 0.8$) are probably due to the fact that models cannot reproduce small-scale convective events that were encountered during the flights (Hegglin, 2004). However, most models underestimate observed data variability ($\sigma f/\sigma r < 1$), probably also related to inability to reproduce small- or regional-scale features in the observations.

4 CONCLUSIONS

Carbon monoxide is a compound with a rather long lifetime in the troposphere. It is emitted by several emission sources, formed by VOC oxidation and transformed to carbon dioxide by oxidation with OH radicals. Furthermore, vertical and horizontal mixing affects its concentrations. We regard the following processes as most critical to explain the partial disagreement between numerical simulations performed within QUANTIFY and available measurements:

- Tropospheric CO concentrations depend on the applied emissions inventories. While model biases are not affected by either the use of preliminary or final QUANTIFY traffic emissions, the agreement between measurements and model results is improved when using the set of POET CO emissions compared to when using QUANTIFY preliminary or final emissions. However, it remains an open question what the cause(s) for the better model performance of the simulation with POET emission is (are). Additionally, the biomass burning emissions inventory used, which is representative for the year 2000 (specifications see Hoor et al., 2009) may not reflect atmospheric conditions in 2003, as it is known that 2002/2003 biomass burning emissions were anomalously high in the extratropical northern hemisphere (e.g., Yurganov et al., 2005).
- CO can be formed from VOC oxidation. This source is expected to be different from model to model adding additional uncertainty in the comparison between simulations and measurements.
- The sharp vertical gradient in CO concentration across the tropopause is an additional challenge for global simulations. The results indicate that current model resolution may be insufficient to resolve this gradient.

In a further study the information from ozone and nitrogen concentrations will be used to shed more light in the reliability of the numerical simulations performed within QUANTIFY.

REFERENCES

Brasseur, G. P., R.A. Cox, D. Hauglustaine, I. Isaksen, J. Lelieveld, D.H. Lister, R. Sausen, U. Schumann, A. Wahner, and P. Wiesen, 1998: European scientific assessment of the effects of aircraft emissions. Atmos. Envir., 32, 2329–2418.

Brunner, D., J. Staehelin, H.L. Rogers, M.O.Köhler, J.A. Pyle, D.A. Hauglustaine, L. Jourdain, T. K. Berntsen, M. Gauss, I. S. A. Isaksen, E. Meijer, P. van Velthoven, G. Pitari, E. Mancini, V. Grewe, and R. Sausen, 2005: An evaluation of the performance of chemistry transport models –Part 2: Detailed comparison with two selected campaigns. Atmos. Chem. Phys., 5, 107–129.

Brunner, D., J. Staehelin, H.L. Rogers, M.O. Köhler, J.A. Pyle, D. Hauglustaine, L. Jourdain, T.K. Berntsen, M. Gauss, I.S.A. Isaksen, E. Meijer, P. van Velthoven, G. Pitari, E. Mancini, V. Grewe, and R. Sausen, 2003: An evaluation of the performance of chemistry transport models by comparison with research aircraft observations. Part 1: Concepts and overall model performance. Atmos. Chem. Phys., 3, 1609-1631.

Engel, A., H. Bönisch, D. Brunner, H. Fischer, H. Franke, G. Günterh, C. Gurk, M. Hegglin, P. Hoor, R. Königstedt, M. Krebsbach, R. Maser, U. Parchatka, T. Peter, D. Schell, C. Schiller, U. Schmidt, N. Spelten, T. Szabo, U. Weers, H. Wernli, T. Wetter, and V. Wirth, 2006: Higly resolved observations of traces gases in the lowermost stratosphere and upper troposphere from the Spurt project: an overview. Atmos. Chem. Phys., 6, 283-301.

Eyers, C., P. Norman, J. Middel, M. Plohr, S. Michot, K. Atkinson, and R. Christou, 2004: AERO2K Global Aviation Emissions Inventories for 2002 and 2025. Tech. Rep. 04/01113, QinetiQ, http://elib.dlr.de/1328.

Hegglin, M.I., 2004: Airborne NOy-, NO- and O3-measurements during SPURT: Implications for atmospheric transport, dissertation, Diss. ETH No. 15553, 209 pp.

Hoor, P., J. Borken-Kleefeld, D. Caro, O. Dessens, O. Endresen, M. Gauss, V. Grewe, D. Hauglustaine, I.S.A. Isaksen, P. Jöckel, J. Lelieveld, E. Meijer, D. Olivie, M. Prather, C. Schnadt Poberaj, J. Staehelin, Q. Tang, J. van Aardenne, P. van Velthoven, and R. Sausen, 2009: The impact of traffic emissions on atmospheric ozone and OH: results from QUANTIFY. Atmos. Chem. Phys., 9, 3113-3136.

IPCC (Intergovernmental Panel on Climate Change), 2001: Climate change 2001: The scientific basis, Contribution of Working Group 1 to the Third Assessment Report, edited by: Houghton, J. T., Cambridge University Press, Cambridge, United Kingdom and New York, NY, USA, 891 pp..

Jöckel, P., H. Tost, A. Pozzer, C. Brühl, J. Buchholz, L. Ganzeveld, P. Hoor, A. Kerkweg, M. Lawrence, R. Sander, B. Steil, G. Stiller, M. Tanharte, D. Taraborrelli, J. van Aardenne, and J. Lelieveld, 2006: Evaluation of the atmospheric chemistry GCM ECHAM5/MESSy: Consistent simulation of ozone in the stratosphere and troposphere. Atmos. Chem. Phys., 6, 5067-5104.

Marenco, A., V. Thouret, P. Nédélec, H. Smit, M. Helten, D. Kley, F. Karcher, P. Simon, K. Law, J. Pyle, G. Poschmann, R. Von Wrede, C. Hume, and T. Cook, 1998: Measurement of ozone and water vapour by Airbus in-service aircraft: The MOZAIC program, An overview. J. Geophys. Res., 103, 25631–25642.

NASA, 1999: Atmospheric Effects of Aviation, A Review of NASA's Subsonic Assessment Project. National Academy Press, Washington, D.C., 41 pp.

Penner, J. E., D. Lister, D. Griggs, D. Docken, and M. MacFarland (Eds), 1999: IPCC Special Report on Aviation and the Global Atmosphere. Cambridge University Press, New York, 373 pp.

Stohl, A. S. Eckhardt, C. Forster, P. James, and N. Spichtinger, 2002: On the pathways and timescales of intercontinental air pollution transport, J. Geophys. Res., 107, D23, 4684, doi:10.1029/2001JD001396.

Taylor, K.E., 2001: Summarizing multiple aspects of model performance in a single diagram. J. Geophys. Res., 106, 7183–7192.

Teyssèdre, H., M. Michou, H. L. Clark, B. Josse, F. Karcher, D. Olivié, V.-H. Peuch, D. Saint-Martin, D. Cariolle, J.-L. Attié, P. Nédélec, P. Ricaud, V. Thouret, R. J. van der A, A. Volz-Thomas, and F. Chéroux, 2007: A new tropospheric and stratospheric Chemistry and Transport Model MOCAGE-Climat for multi-year studies: evaluation of the present-day climatology and sensitivity to surface processes. Atmos. Chem. Phys., 7, 5815–5860.

Yurganov, L.N., P. Duchatelet, A. V. Dzhola, D. P. Edwards, F. Hase, I. Kramer, E. Mahieu, J. Mellqvist, J. Notholt, P. C. Novelli, A. Rockmann, H. E. Scheel, M. Schneider, A. Schulz, A. Strandberg, R. Sussmann, H. Tanimoto, V. Velazco, J. R. Drummond, and J. C. Gille, Increased Northern Hemispheric carbon monoxide burden in the troposphere in 2002 and 2003 detected from the ground and from space, Atmos. Chem. Phys., 5, 563–573.